Universitat de Barcelona

Tutorial sesion:

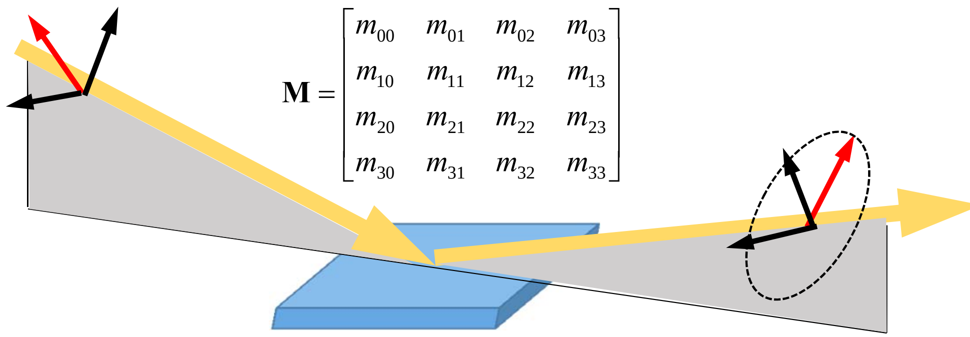

$$\mathbf{M} = \begin{bmatrix} m_{00} & m_{01} & m_{02} & m_{03} \\ m_{10} & m_{11} & m_{12} & m_{13} \\ m_{20} & m_{21} & m_{22} & m_{23} \\ m_{30} & m_{31} & m_{32} & m_{33} \end{bmatrix}$$

Mueller Matrix Ellipsometry

Oriol Arteaga
Dep. Applied Physics and Optics
University of Barcelona

9TH WORKSHOP ELLIPSOMETRY @ UTWENTE

Outline

- Historical introduction
- Basic concepts about Mueller matrices
- Mueller matrix ellipsometry instrumentation
- Further insights. Measurements and simulations
- Symmetries and asymmetries of the Mueller matrix. Relation to anisotropy.
- Applications and examples
- Concluding remarks

Historical introduction

Historical introduction

G G. Stokes
in 1852

Stokes Parameters

90 years, **almost** forgotten!

Francis Perrin
in 1942

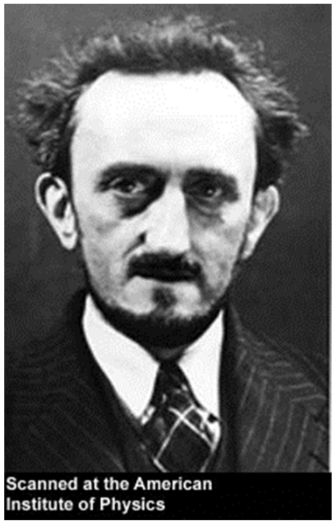

F. Perrin, J. Chem. Phys. 10, 415 (1942).
Translation from the french:
F. Perrin, J. Phys. Rad. 3, 41 (1942)

Historical introduction

1852
G G. Stokes (1819-1903)

Stokes Parameters

1929
Paul Soleillet (1902-1992)

P. Soleillet, Ann. Phys. 12, 23 (1929)

SUR LES PARAMÈTRES CARACTÉRISANT LA POLARISATION PARTIELLE DE LA LUMIÈRE DANS LES PHÉNOMÈNES DE FLUORESCENCE

On en conclut que μ', ν', γ', σ' sont des fonctions linéaires et homogènes de μ, ν, γ, σ et que de même I′, M′, C′, S′ sont des fonctions linéaires et homogènes de I, M, C, S.

1942
Francis Perrin (1901-1992)

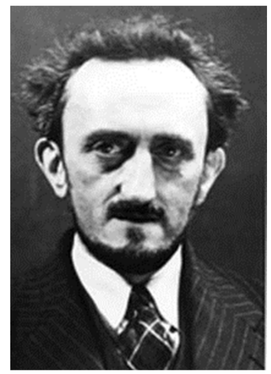

F. Perrin, J. Phys. Rad. 3, 41 (1942)

G′. Since the Stokes' parameters are additive for the superposition of non-coherent beams, this requires that the quantities I'_1, M'_1, C'_1, S'_1 be linear homogeneous functions of the quantities I_1, M_1, C_1, S_1, i.e., that

$$\begin{aligned} I'_1 &= a_{11}I_1+a_{12}M_1+a_{13}C_1+a_{14}S_1,\\ M'_1 &= a_{21}I_1+a_{22}M_1+a_{23}C_1+a_{24}S_1,\\ C'_1 &= a_{31}I_1+a_{32}M_1+a_{33}C_1+a_{34}S_1,\\ S'_1 &= a_{41}I_1+a_{42}M_1+a_{43}C_1+a_{44}S_1. \end{aligned} \quad (33)$$

1943
Hans Mueller (1900-1965)

K. Järrendahl and B. Kahr, Woollam newsletter, February 2011, pp. 8–9

H. Mueller, Report no. 2 of OSR project OEMsr-576 (1943)

The writer knows of no textbook in which these mathematical methods are discussed. Certain aspects of the method discussed here are given by F. Perrin, Journal of Chemical Physics 10 415 (1942) where older references may be found.

Historical introduction

- P. S. Hauge, Opt. Commun. 17, 74 (1976).
- R. M. A. Azzam, Opt. Lett. **2**, 148-150 (1978).

Instrumental papers about the dual rotating compensator technique

"Generalized ellipsometry"

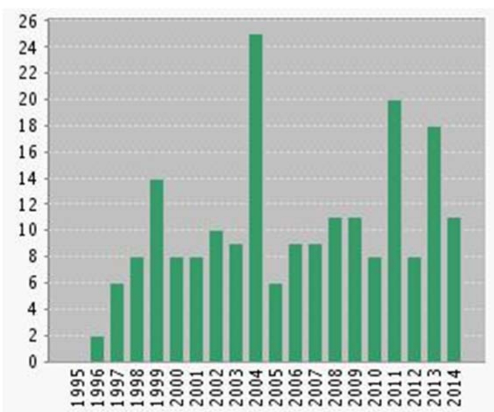

"Mueller matrix ellipsometry"

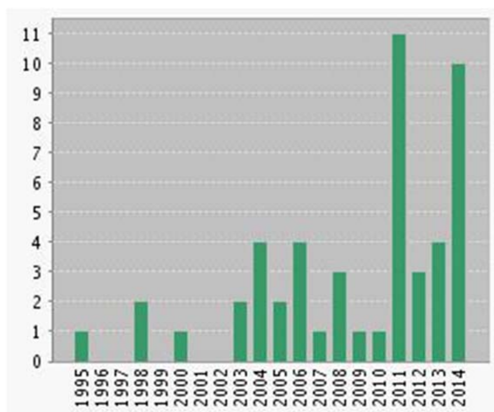

"Mueller matrix spectroscopic ellipsometry"

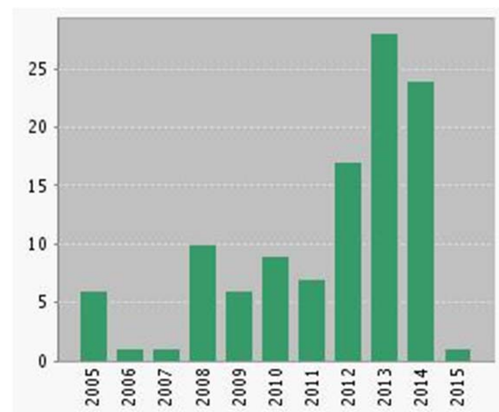

Web of Science Citation Reports

Basic concepts about Mueller matrices

Basic concepts about Mueller matrices

$$\mathbf{S} = \begin{bmatrix} I \\ Q \\ U \\ V \end{bmatrix} = \begin{bmatrix} S_0 \\ S_1 \\ S_2 \\ S_3 \end{bmatrix} = \begin{bmatrix} I \\ I_x - I_y \\ I_{45} - I_{135} \\ I_+ - I_- \end{bmatrix} = \begin{bmatrix} I \\ Ip\cos(2\varphi)\cos(2\chi) \\ Ip\cos(2\varphi)\sin(2\chi) \\ Ip\sin(2\varphi) \end{bmatrix}$$

I Intensity
p Degree of polarization
χ Azimuth
φ Ellipticity

No depolarization: $I = \sqrt{Q^2 + U^2 + V^2}$

$$\mathbf{S}_{out} = \mathbf{M}\mathbf{S}_{in} \qquad \mathbf{M} = \begin{bmatrix} m_{00} & m_{01} & m_{02} & m_{03} \\ m_{10} & m_{11} & m_{12} & m_{13} \\ m_{20} & m_{21} & m_{22} & m_{23} \\ m_{30} & m_{31} & m_{32} & m_{33} \end{bmatrix}$$

Phenomenological description of any scattering experiment

Basic concepts about Mueller matrices. No depolarization

A nondepolarizing Mueller matrix is called a **Mueller-Jones** matrix

Equivalence

$$\mathbf{S}_{out} = \mathbf{M}\mathbf{S}_{in} \quad \Longleftrightarrow \quad \mathbf{E}_{out} = \mathbf{J}\mathbf{E}_{in}$$

M is 4x4 real $\Longleftrightarrow$ $\mathbf{J} = \begin{bmatrix} r_{pp} & r_{ps} \\ r_{sp} & r_{ss} \end{bmatrix}$ is 2x2 complex matrix

A Jones or Mueller-Jones Jones depends on 6-7 parameters.

But note that the 16 elements of a Mueller-Jones matrix can be still all different!

Transformation

$$\mathbf{M} = \mathbf{T}(\mathbf{J} \otimes \mathbf{J}^*)\mathbf{T}^{-1} \qquad \mathbf{T} = \begin{bmatrix} 1 & 0 & 0 & 1 \\ 1 & 0 & 0 & -1 \\ 0 & 1 & 1 & 0 \\ 0 & i & -i & 0 \end{bmatrix}$$

Basic concepts about Mueller matrices. No depolarization and isotropy

All modern ellipsometers measure elements of the Mueller matrix.

This is a common representation for isotropic media:

$$\mathbf{J}_{sample} = \begin{bmatrix} r_p & 0 \\ 0 & r_s \end{bmatrix}$$

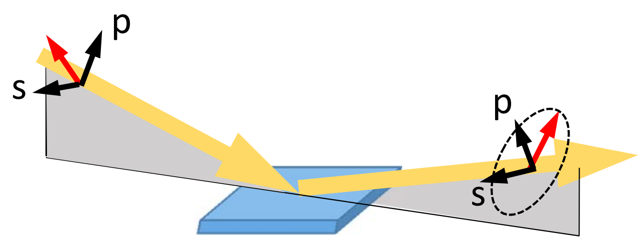

$$\mathbf{M}_{sample} = \begin{bmatrix} 1 & -N & 0 & 0 \\ -N & 1 & 0 & 0 \\ 0 & 0 & C & S \\ 0 & 0 & -S & C \end{bmatrix}$$

$$N = \cos(2\psi)$$
$$S = \sin(2\psi)\sin(\Delta)$$
$$C = \sin(2\psi)\cos(\Delta)$$
$$N^2 + S^2 + C^2 = 1$$

Standard ellipsometry:

- Thickness measurements of thin films
- Optical functions of isotropic materials

$$\rho = (\rho_{real} + i\rho_{imag}) = \frac{r_p}{r_s} = \tan(\psi)e^{i\Delta} = \frac{C + iS}{1 + N}$$

This Mueller matrix depends only on 2 parameters

Basic concepts about Mueller matrices. Depolarization

Depolarization is the reduction of the degree of polarization of light. Typically occurs when the emerging light is composed of several incoherent contributions.

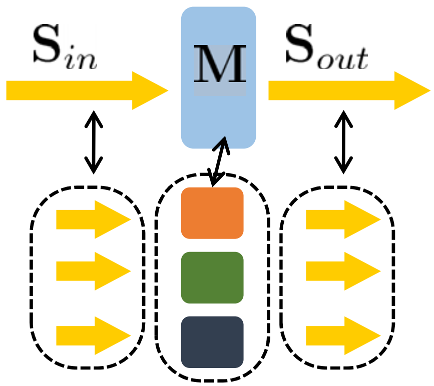

Reasons:

Sample exhibits spatial, temporal or frequency heterogeneity over the illuminated area

Quantification of the depolarization: Depolarization index (DI)

$$DI = \frac{\sqrt{\sum_{ij} m_{ij}^2 - m_{00}^2}}{\sqrt{3} m_{00}}$$

$$0 \leq DI \leq 1$$

The DI of a Mueller-Jones matrix is 1

J. J. Gil, E. Bernabeu, Opt. Acta 32 (1985) 259

Mueller matrix ellipsometry instrumentation

Mueller matrix ellipsometry instrumentation

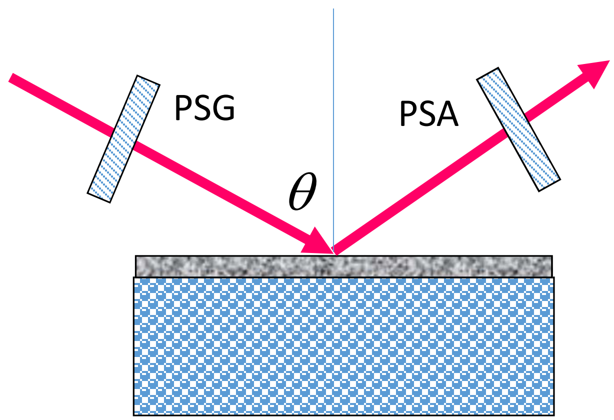

- Polarization state generator: PSG
- Polarization state analyzer: PSA

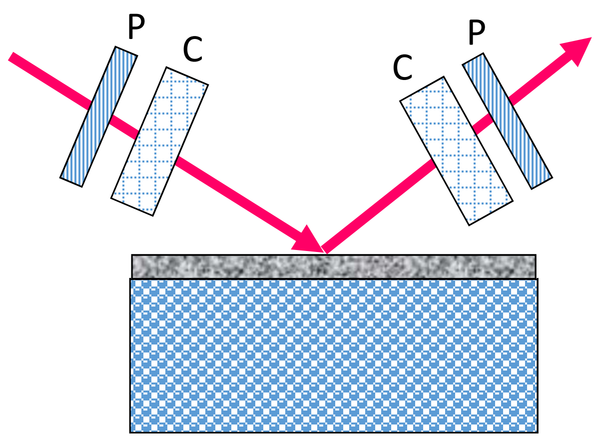

In a MM ellipsometer the PSG and PSA typically contain:

- A polarizer (P)
- A compensating or retarding element (C)

One exception: division-of-amplitude ellipsometers

Mueller matrix ellipsometry instrumentation

The compensating element is the main difference between different types of Mueller matrix ellipsometers

Rotating Retarders P. S. Hauge, J. Opt. Soc. Am. **68**, 1519-1528 (1978)	 	• Fixed Retardation • Changing azimuth	• Waveplates are not very acromatic • Fresnel rohms are hard to rotate • Mechanical rotation
Liquid cristal cells E. Garcia-Caurel et al. Thin Solid Films 455 120-123 (2004).		• Variable Retardation (nematic LC) • Changing azimuth (ferroelectric LC)	• Not transparent in the UV • Temperature dependence • No frequency domain analysis
Piezo-optic modulators (photoelastic modulators) O. Arteaga et al. Appl. Optics 51.28 6805-6817 (2012).	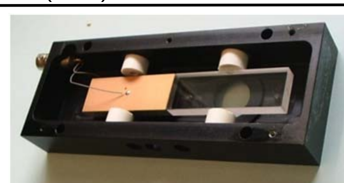	• Variable Retardation • Fixed azimuth	• Two PEMs for each PSG or PSA • Too fast for imaging
Electro-optic modulators (Pockels cells) R. C. Thompson et al. Appl. Opt. 19, 1323–1332 (1980).		• Variable Retardation • Fixed azimuth	• Two cells for each PSG or PSA • Small acceptance angle • Too fast for imaging

Mueller matrix ellipsometry instrumentation

The PSA and PSG of Mueller matrix ellipsometers are no different from other Mueller matrix polarimetric approaches

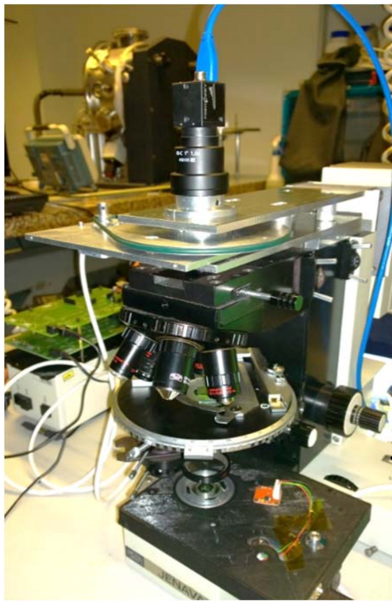

Mueller matrix microscope with two rotating compensators

O. Arteaga et al, Appl. Opt. 53, 2236-2245 (2014)

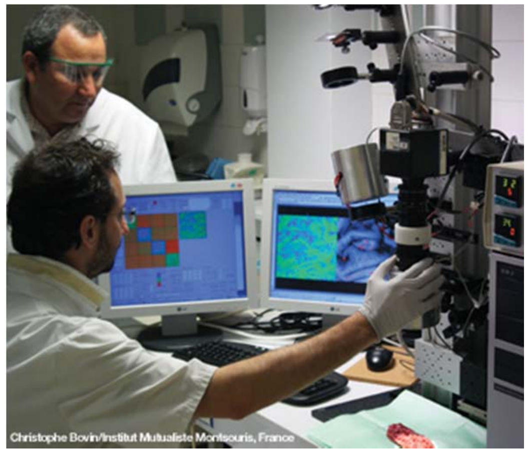

Normal-incidence reflection imaging based on liquid crystals

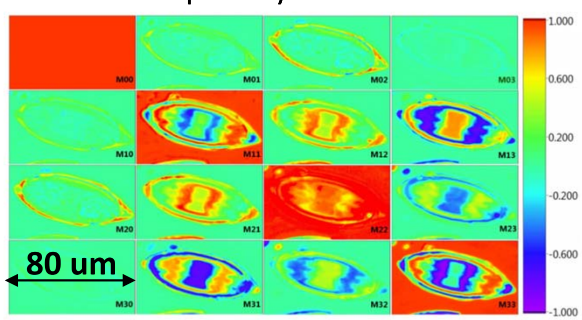

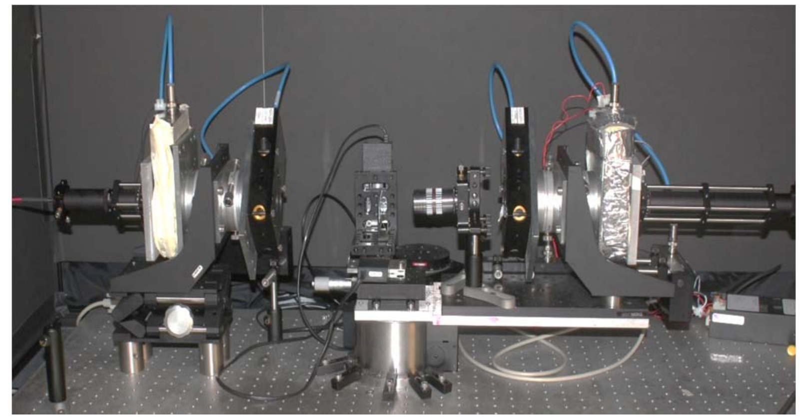

spectroscopic polarimeter based on four photoelastic modulators

Instrumentally wise no different from a MM ellipsometer. Lots of imaging applications in chemistry, medicine, biology, geology, etc.

Further insights
Measurement and simulations

Further insights. Measurement and simulations

A spectroscopic Mueller matrix ellipsometer produces this type of data:

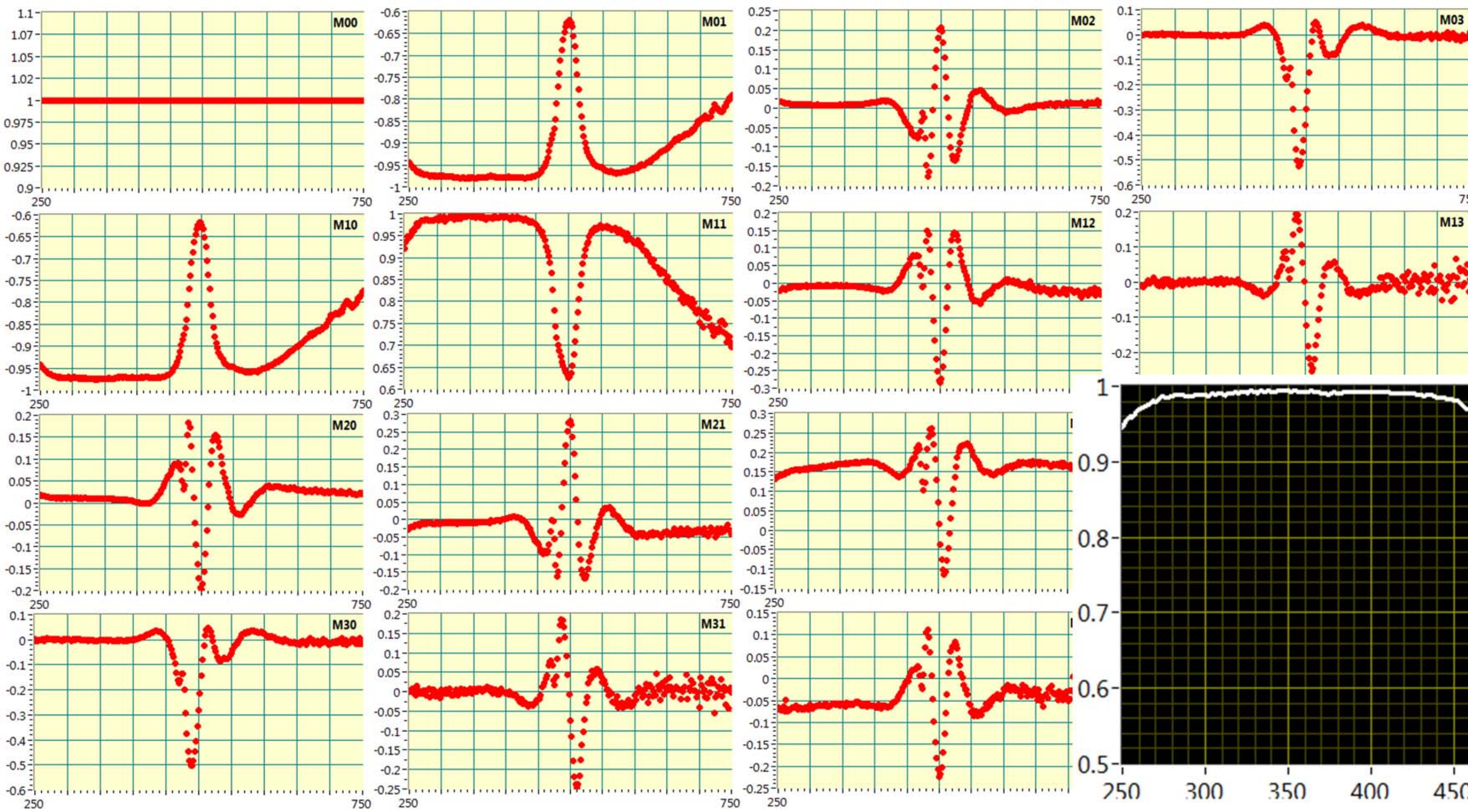

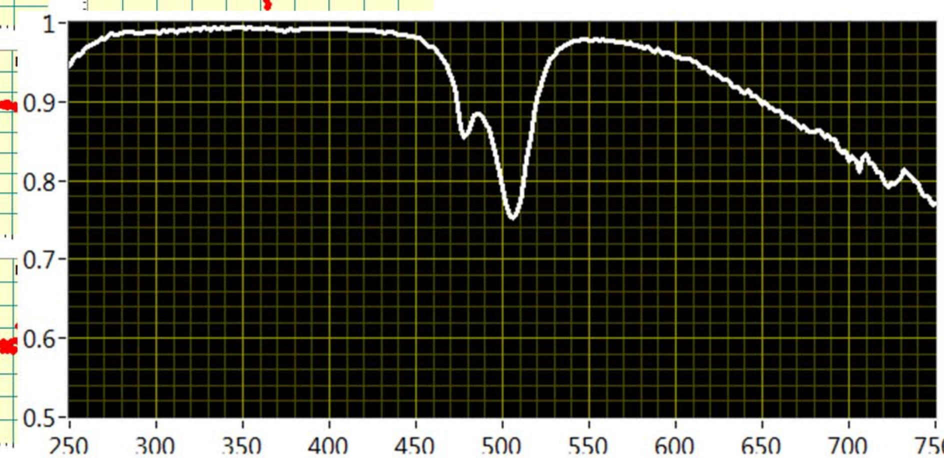

Is this MM depolarizing?

If the depolarization is not significative we can find a proper non-depolarizing estimate

Further insights. Measurement and simulations

Measurement: Mueller matrix ⟷ Simulation usually generates a Jones/Mueller-Jones matrix (coherent model)

Objective: Finding a good nondepolarizing estimate (a Mueller-Jones matrix) for a experimental Mueller matrix

One option,

$$\delta^2 = \sum_{i,j} \left(\mathbf{M}_{ij} - \mathbf{M}_{\mathbf{J}ij}\right)^2 \rightarrow \min$$

Cloude estimate using the Cloude sum decomposition

$$\mathbf{M} = \lambda_0 \mathbf{M}_{\mathbf{J}0} + \lambda_1 \mathbf{M}_{\mathbf{J}1} + \lambda_2 \mathbf{M}_{\mathbf{J}2} + \lambda_3 \mathbf{M}_{\mathbf{J}3}$$

$$\mathbf{M} \approx \lambda_0 \mathbf{M}_{\mathbf{J}0}$$

S. R. Cloude, Optik 75, 26 (1986).
R. Ossikovski, Opt. Lett. **37**, 578-580 (2012).

Further insights. Measurement and simulations. Example

Experimental Mueller matrix

1	-0.6125	0.3377	-0.2466
-0.5766	0.7387	0.0096	0.4076
0.3778	-0.1007	0.6254	-0.3359
0.2536	-0.4551	0.3205	0.3956

$$DI = \frac{\sqrt{\sum_{ij} m_{ij}^2 - m_{00}^2}}{\sqrt{3}m_{00}} = 0.963$$

1. Calculate the Coherency matrix

$$\begin{aligned}
h_{00} &= (m_{00} + m_{11} + m_{22} + m_{33})/4, & h_{01} &= (m_{01} + m_{10} - im_{23} + im_{32})/4, \\
h_{02} &= (m_{02} + m_{20} + im_{13} - im_{31})/4, & h_{03} &= (m_{03} - im_{12} + im_{21} + m_{30})/4, \\
h_{10} &= (m_{01} + m_{10} + im_{23} - im_{32})/4, & h_{11} &= (m_{00} + m_{11} - m_{22} - m_{33})/4, \\
h_{12} &= (im_{03} + m_{12} + m_{21} - im_{30})/4, & h_{13} &= (-im_{02} + im_{20} + m_{13} + m_{31})/4, \\
h_{20} &= (m_{02} + m_{20} - im_{13} + im_{31})/4, & h_{21} &= (-im_{03} + m_{12} + m_{21} + im_{30})/4, \\
h_{22} &= (m_{00} - m_{11} + m_{22} - m_{33})/4, & h_{23} &= (im_{01} - im_{10} + m_{23} + m_{32})/4, \\
h_{30} &= (m_{03} + im_{12} - im_{21} + m_{30})/4, & h_{31} &= (im_{02} - im_{20} + m_{13} + m_{31})/4, \\
h_{32} &= (-im_{01} + im_{10} + m_{23} + m_{32})/4, & h_{33} &= (m_{00} - m_{11} - m_{22} + m_{33})/4.
\end{aligned}$$

Coherency matrix, H

0.7056 +0 i	-0.3318 -0.2896i	0.0468 +0.0713 i	0.0032 -0.0254 i
-0.3318 +0.2896i	0.1601 +0 i	0.038 -0.015 i	0.0097 +0.0043 i
0.0468 -0.0713 i	0.038 +0.015 i	0.1288 +0 i	-0.022 +0.0192 i
0.0032 +0.0254 i	0.0097 -0.0043 i	-0.022 -0.0192 i	0.0055 +0 i

2. Calculate the eigenvectors of H (is a hermitian matrix, so eigenvectors are real)

$\lambda_0 = 0.972$ $\quad \lambda_2 = 0.009$

$\lambda_1 = 0.022$ $\quad \lambda_3 = -0.003$

$$\mathbf{M} = \lambda_0 \mathbf{M}_{\mathbf{J}0} + \lambda_1 \mathbf{M}_{\mathbf{J}1} + \lambda_2 \mathbf{M}_{\mathbf{J}2} + \lambda_3 \mathbf{M}_{\mathbf{J}3}$$

$$\mathbf{M} \approx \lambda_0 \mathbf{M}_{\mathbf{J}0}$$

Further insights. Measurement and simulations. Example

3. The eigenvector corresponding to λ_0 defines the Jones matrix corresponding to $\mathbf{M}_{\mathbf{J}0}$

$$r_{pp} = \Psi_0 + \Psi_1 \qquad r_{ps} = \Psi_2 - i\Psi_3$$

$$r_{sp} = \Psi_2 + i\Psi_3 \qquad r_{ss} = \Psi_0 - \Psi_1$$

Jones matrix

0.465 -0.1959 i	0.2436 -0.2603 i
0.1786 -0.2497 i	1.173 +0.1959 i

Initial Experimental Mueller matrix

1	-0.6125	0.3377	-0.2466
-0.5766	0.7387	0.0096	0.4076
0.3778	-0.1007	0.6254	-0.3359
0.2536	-0.4551	0.3205	0.3956

Best nondepolarizing estimate

1	-0.630ε	0.3438	-0.269:
-0.596	0.7657	0.0039:	0.4245
0.3881	-0.108‚	0.6513	-0.354ε
0.2878	-0.459ξ	0.3244	0.4216

Suitable to compare with coherent models

Further insights. Measurement and simulations. Expressing non-depolarizing data

$$\mathbf{J} = \begin{bmatrix} r_{pp} & r_{ps} \\ r_{sp} & r_{ss} \end{bmatrix}$$

1 | 2

$$\rho = \frac{r_{pp}}{r_{ss}} = \tan(\psi)e^{i\Delta}$$

$$\rho_{ps} = \frac{r_{ps}}{r_{ss}} = \tan(\psi_{ps})e^{i\Delta_{ps}}$$

$$\rho_{ps} = \frac{r_{sp}}{r_{ss}} = \tan(\psi_{sp})e^{i\Delta_{sp}}$$

3

$$L = LB - iLD = i\Omega(\rho - 1)$$

$$L' = LB' - iLD' = i\Omega(\rho_{ps} + \rho_{sp})$$

$$C = CB - iCD = \Omega(\rho_{ps} - \rho_{sp})$$

$$\Omega = \frac{TK}{\sin(T)}$$

$$T = \cos^{-1}[K(\rho + 1)/2]$$

$$K = [\rho - \rho_{ps}\rho_{sp}]^{-1/2}$$

This notation is very suitable for normal-incidence transmission and reflection data:
CD: circular dichroism/diatt.
CB: circular birefrigence/retard.
LD: horiz. linear dichroism/diatt.
... etc

O. Arteaga & A. Canillas, Opt. Lett. **35**, 559-561 (2010)

For the previous example:

1

$$\rho = 0.359 - 0.227i$$
$$\rho_{ps} = 0.166 - 0.250i$$
$$\rho_{sp} = 0.114 - 0.231i$$

2

$$\psi = 23.0^{o} \quad \Delta = -32.3^{o}$$
$$\psi_{ps} = 16.7^{o} \quad \Delta_{ps} = -56.4^{o}$$
$$\psi_{sp} = 14.5^{o} \quad \Delta_{sp} = -63.9^{o}$$

3

$$CD = 0.012 \quad CB = 0.082$$
$$LD = 0.885 \quad LB = 0.510$$
$$LD' = -0.544 \quad LB' = 0.635$$

Mueller matrix symmetries and anisotropy

Mueller matrix symmetries and anisotropy

In the **isotropic** case

$$\mathbf{M} = \begin{bmatrix} 1 & m_{01} & 0 & 0 \\ m_{01} & 1 & 0 & 0 \\ 0 & 0 & m_{22} & m_{23}* \\ 0 & 0 & -m_{23}* & m_{22} \end{bmatrix} \qquad \mathbf{J} = \begin{bmatrix} r_p & 0 \\ 0 & r_s \end{bmatrix} \tag{1}$$

The MM elements with an asteriks vanish in absence of absorption and **J** is real (asumming semi-infinite substrate as a sample)

But this symmetry also applies to some situations with anisotropy!

Uniaxial

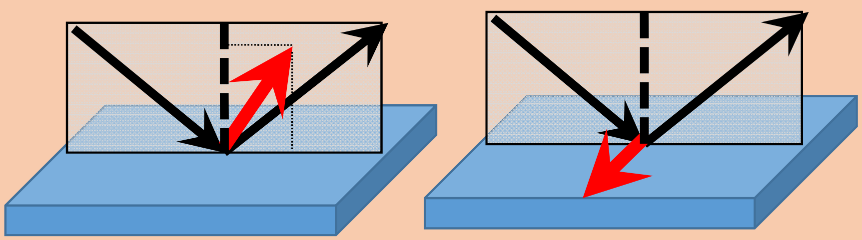

Biaxial (orthorombic)

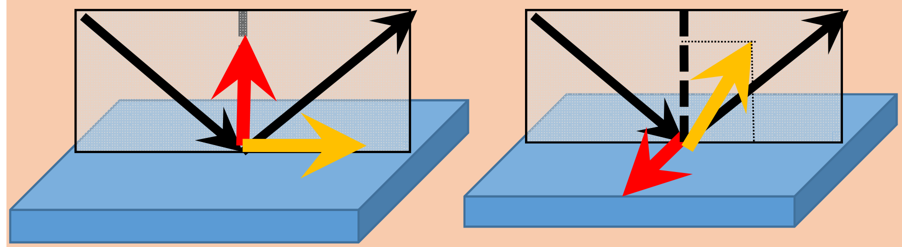

Arrows are O. A.

Biaxial (monoclinic)

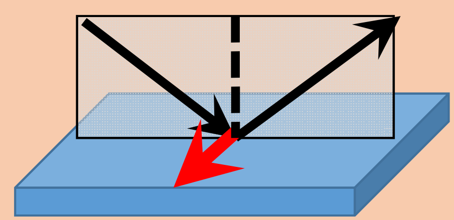

Arrow is P. A.

Mueller matrix symmetries and anisotropy

2

$$\mathbf{M} = \begin{bmatrix} 1 & m_{01} & m_{02} & m_{03}\,* \\ m_{01} & m_{11} & m_{12} & m_{13}\,* \\ -m_{02} & -m_{12} & m_{22} & m_{23}\,* \\ m_{03}\,* & m_{13}\,* & -m_{23}\,* & m_{33} \end{bmatrix} \quad \mathbf{J} = \begin{bmatrix} r_{pp} & r_{ps} \\ -r_{ps} & r_{ss} \end{bmatrix}$$

The MM elements with an asteriks vanish in absence of absorption and **J** is real (asumming semi-infinite substrate as a sample)

Uniaxial

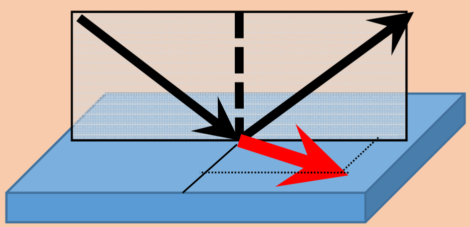

Arrows are O. A.

Biaxial (orthorombic)

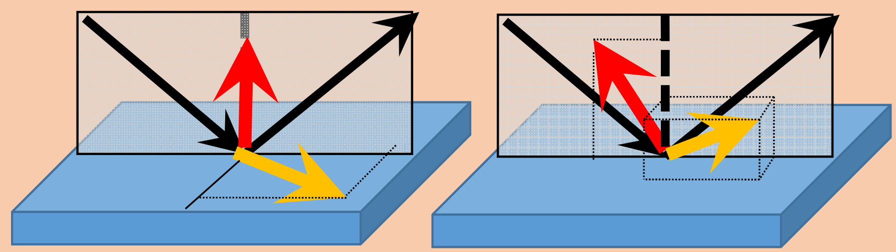

Biaxial (monoclinic)

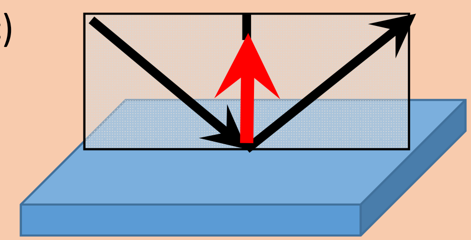

Arrow is P. A.

Mueller matrix symmetries and anisotropy

3 $$\mathbf{M} = \begin{bmatrix} 1 & m_{01} & m_{02} & m_{03}* \\ m_{01} & m_{11} & m_{12} & m_{13}* \\ m_{02} & m_{12} & m_{22} & m_{23}* \\ -m_{03}* & -m_{13}* & -m_{23}* & m_{33} \end{bmatrix} \quad \mathbf{J} = \begin{bmatrix} r_{pp} & r_{ps} \\ r_{ps} & r_{ss} \end{bmatrix}$$

The MM elements with an asteriks vanish in absence of absorption and **J** is real (asumming semi-infinite substrate as a sample)

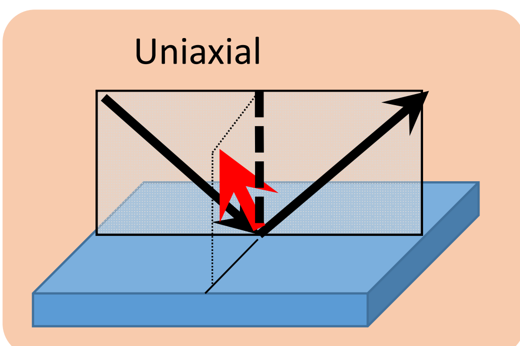

Arrow is O. A.

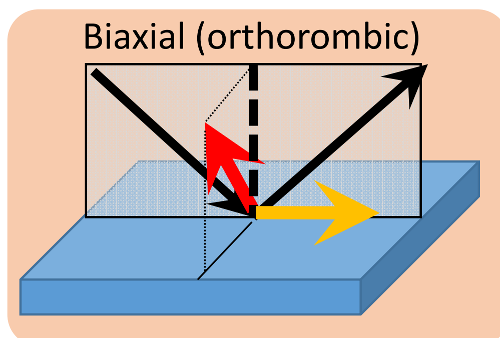

Arrows are O. A.

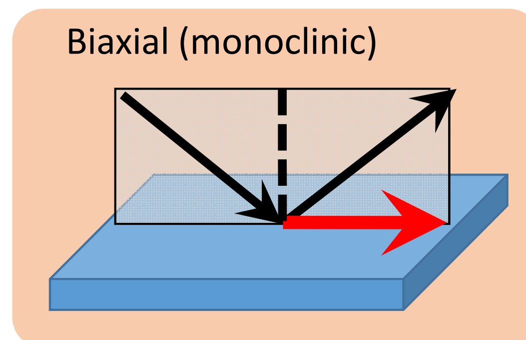

Arrow is P. A.

Mueller matrix symmetries and anisotropy

4

$$\mathbf{M} = \begin{bmatrix} 1 & m_{01} & m_{02}* & m_{03} \\ m_{01} & m_{11} & m_{12}* & m_{13} \\ -m_{02}* & -m_{12}* & m_{22} & m_{23} \\ m_{03} & m_{13} & -m_{23}* & m_{33} \end{bmatrix} \quad \mathbf{J} = \begin{bmatrix} r_{pp} & r_{ps} \\ -r_{ps} & r_{ss} \end{bmatrix}$$

The MM elements with an asteriks vanish in absence of absorption and **J** is imaginary (asumming semi-infinite substrate as a sample)

Bi-isotropic media

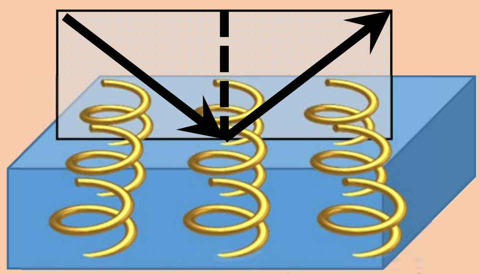

Applications and examples

Applications and examples. A general idea about anisotropy

Instrinsic anisotropy vs structural/form anisotropy

$$\mathbf{M} = \begin{bmatrix} m_{00} & m_{01} & m_{02} & m_{03} \\ m_{10} & m_{11} & m_{12} & m_{13} \\ m_{20} & m_{21} & m_{22} & m_{23} \\ m_{30} & m_{31} & m_{32} & m_{33} \end{bmatrix}$$

Expect small values of these elements for intrinsic anisotropy

E.g. Reflection on a calcite substrate

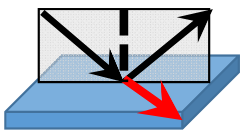

AOI 65°

$\varepsilon_o = 2.749$

$\varepsilon_e = 2.208$

1	-0.8864	-0.08172	0
-0.8864	0.9877	0.1331	0
0.08172	-0.1331	0.4434	0
0	0	0	0.4557

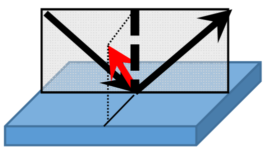

1	-0.9504	0.1038	0
-0.9504	0.9917	-0.07624	0
0.1038	-0.07624	0.3016	0
0	0	0	0.2933

Applications. Dielectric tensor of crystals

Measure the complex dielectric function (DF) tensor above and below the band edge

$$D_i = \varepsilon_{ij}(\lambda)E_j$$

The dielectric tensor is symmetric

$$\boldsymbol{\varepsilon} = \begin{bmatrix} \varepsilon_{11} & \varepsilon_{12} & \varepsilon_{13} \\ \varepsilon_{12} & \varepsilon_{22} & \varepsilon_{23} \\ \varepsilon_{13} & \varepsilon_{23} & \varepsilon_{33} \end{bmatrix}$$

A magnetic field breaks the symmetry. E.g. MOKE

$$\boldsymbol{\varepsilon}' = \mathbf{A}\boldsymbol{\varepsilon}\mathbf{A}^{\mathrm{T}}$$

$$\mathbf{A}(\alpha,\beta,\gamma) = \begin{bmatrix} C_\alpha C_\gamma - C_\beta S_\alpha S_\gamma & -C_\alpha S_\gamma - C_\beta C_\gamma S_\alpha & S_\alpha S_\beta \\ C_\gamma S_\alpha + C_\alpha C_\beta S_\gamma & C_\alpha C_\beta C_\gamma - S_\alpha S_\gamma & -C_\alpha S_\beta \\ S_\beta S_\gamma & C_\gamma S_\beta & C_\beta \end{bmatrix}$$

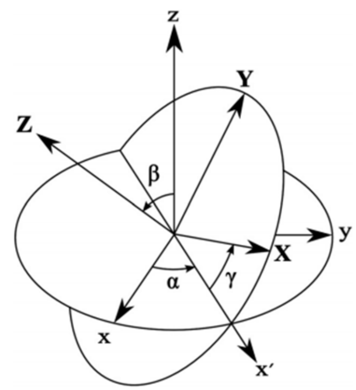

The principal values of the tensor correspond to crystal symmetry directions for isotropic, uniaxial and orthorhombic materials

Berreman's 4x4 complex formalism is used to calculate ρ, ρ_{sp} and ρ_{ps} from elements of $\boldsymbol{\varepsilon}$ and the angle of incidence (a fully analytical treatment is sometimes possible).

Applications. Dielectric tensor of crystals

General scheme of the approach:

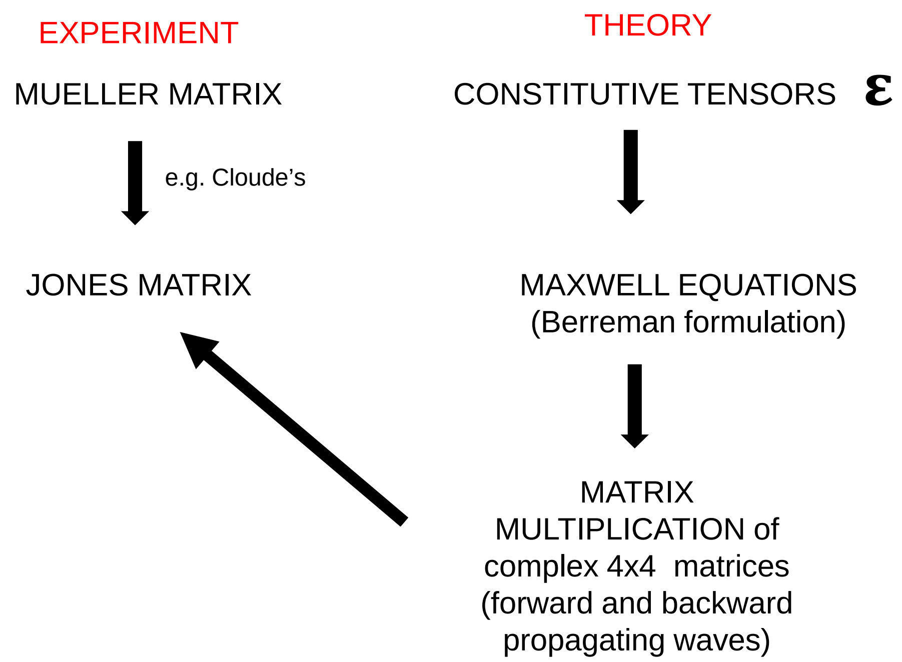

Applications. Dielectric tensor of crystals

Rutile (Uniaxial)

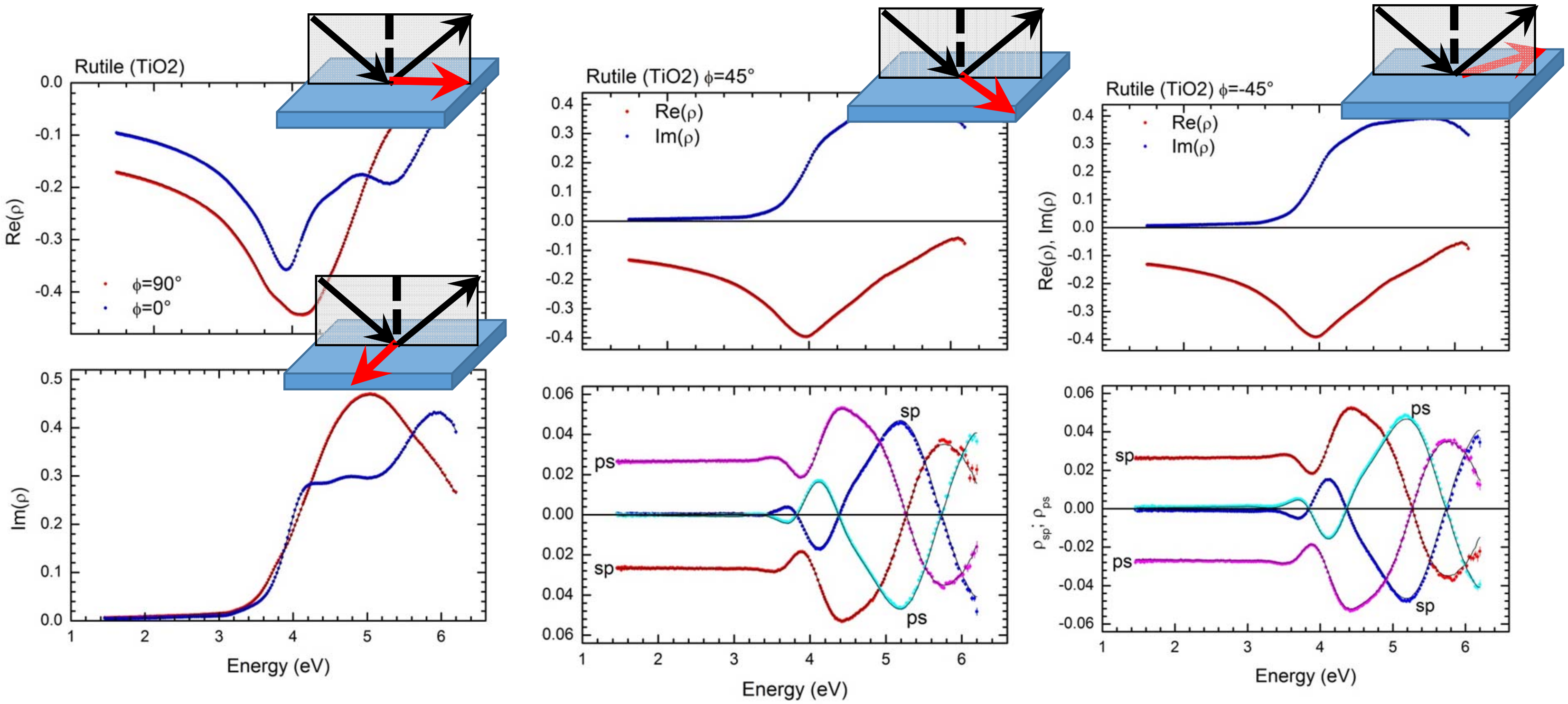

G. E. Jellison, F. A. Modine, and L. A. Boatner, Opt. Lett. 22, 1808 (1997).
Jellison and Baba, J. Opt. Soc. Am. 23, 468 (2006).

Applications. Dielectric tensor of crystals

Rutile (Uniaxial)

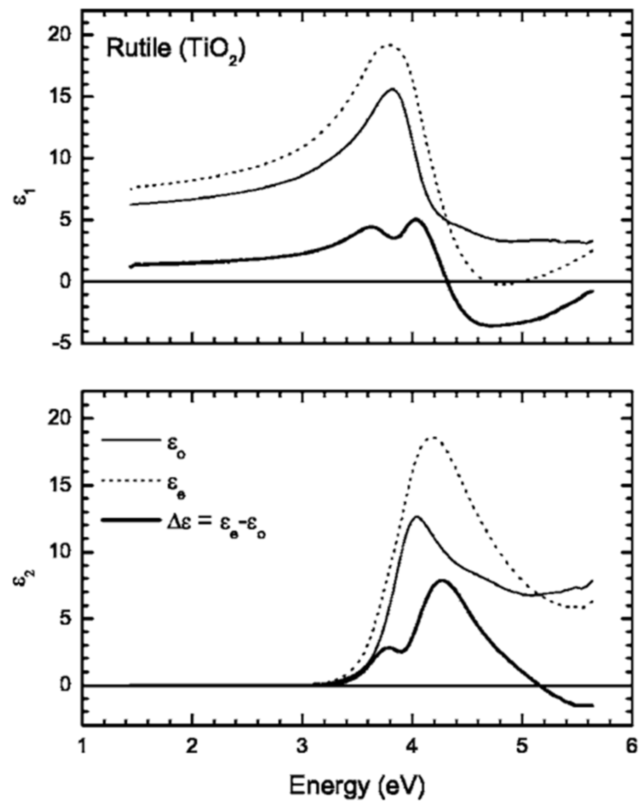

$$\boldsymbol{\varepsilon} = \begin{bmatrix} \varepsilon_{11} & \varepsilon_{12} & 0 \\ \varepsilon_{12} & \varepsilon_{22} & 0 \\ 0 & 0 & \varepsilon_{33} \end{bmatrix}$$

Applications. Dielectric tensor of crystals

Monoclinic $CdWO_4$

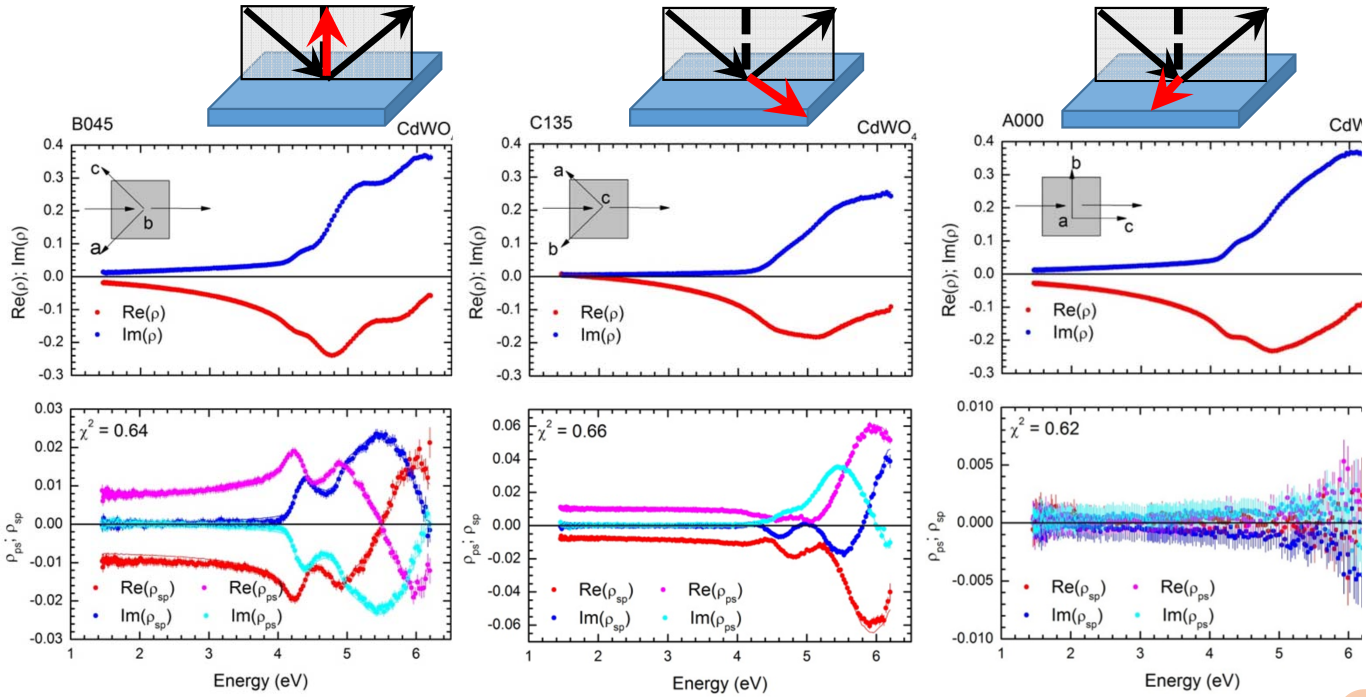

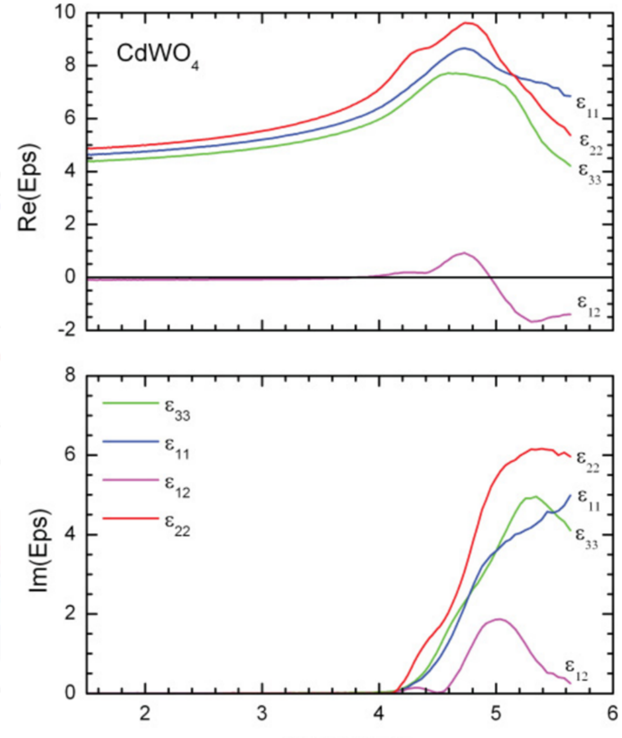

Jellison, McGuire, Boatner, Budai, Specht, and Singh, *Phys. Rev. B* **84**, 195439 (2011).

Note that a non-diagonal dielectric tensor can led to a block diagonal MM

Mueller matrix Scatterometry

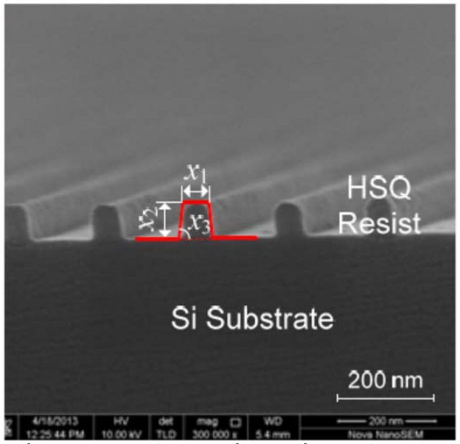

e-beam patterned grating structure

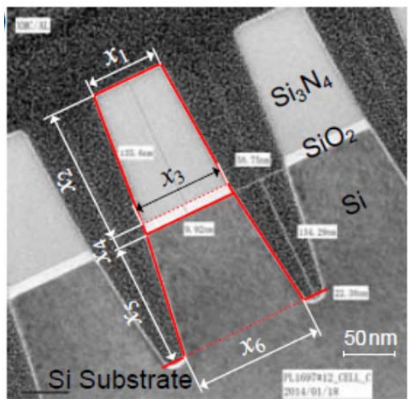

Trench nanostructure encountered in the manufacturing of flash memory storage cells

(Form anisotropy)

Measurements in periodic grating-like structures
Analysis of the Zeroth-order diffracted light (specular reflection).

$$n_2 \sin(\theta_m) = n_i \sin(\theta_i) - m\frac{\lambda}{P}$$

Qualitative understanding of the measurements is posible attending to MM symmetries, and Rayleigh anomalies of higher orders. Energy distribution to higher orders

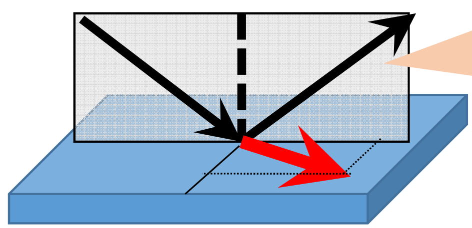

Expect the same symmetries as for a sample with optic axis lying in the plane of the sample

Rigorous-coupled wave analysis (RCWA). Field components expanded into Fourier series

Mueller matrix Scatterometry

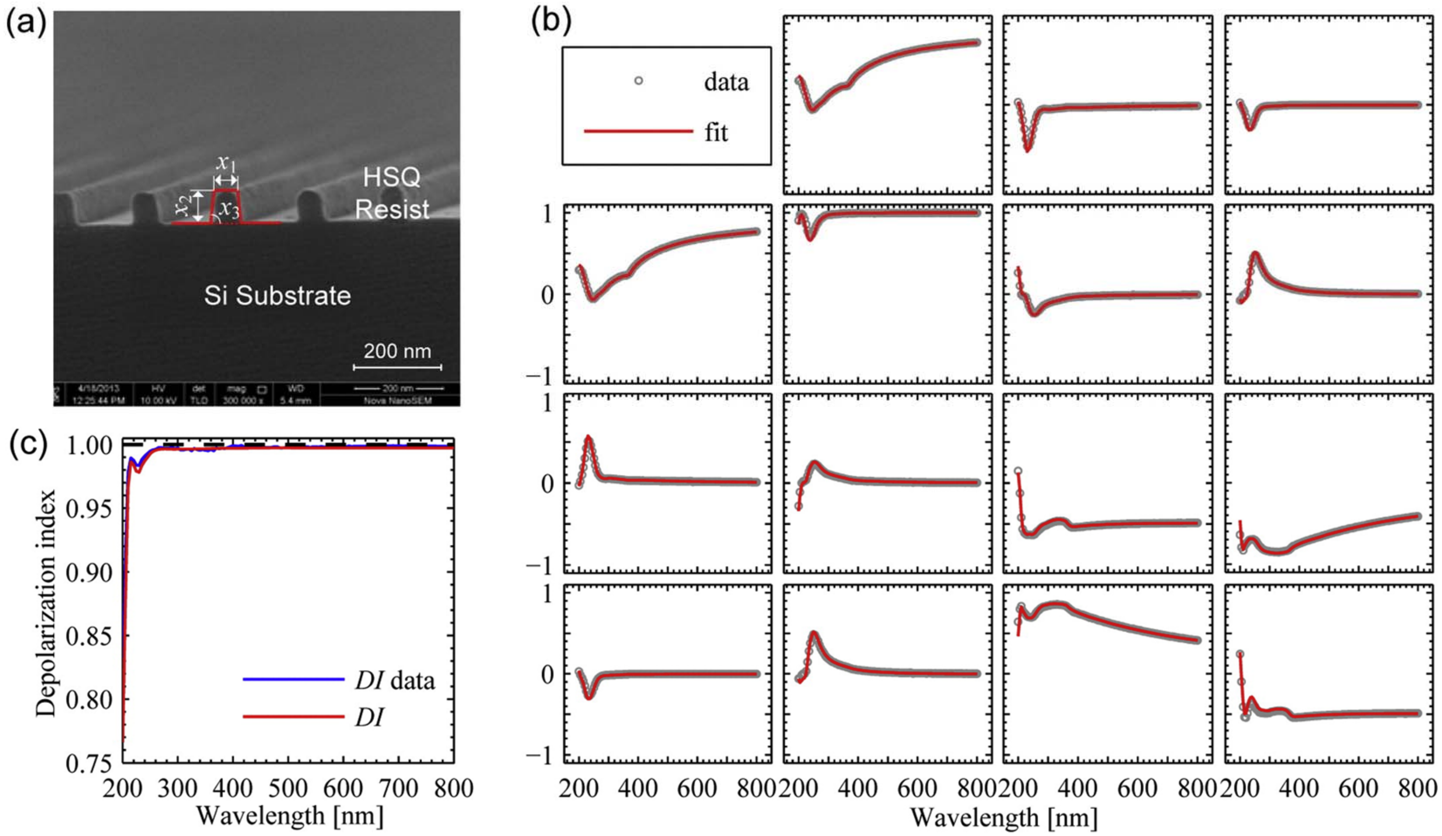

S. Liu, et al., Development of a broadband Mueller matrix ellipsometer as a powerful tool for nanostructure metrology, Thin Solid Films , in press

Mueller matrix Scatterometry

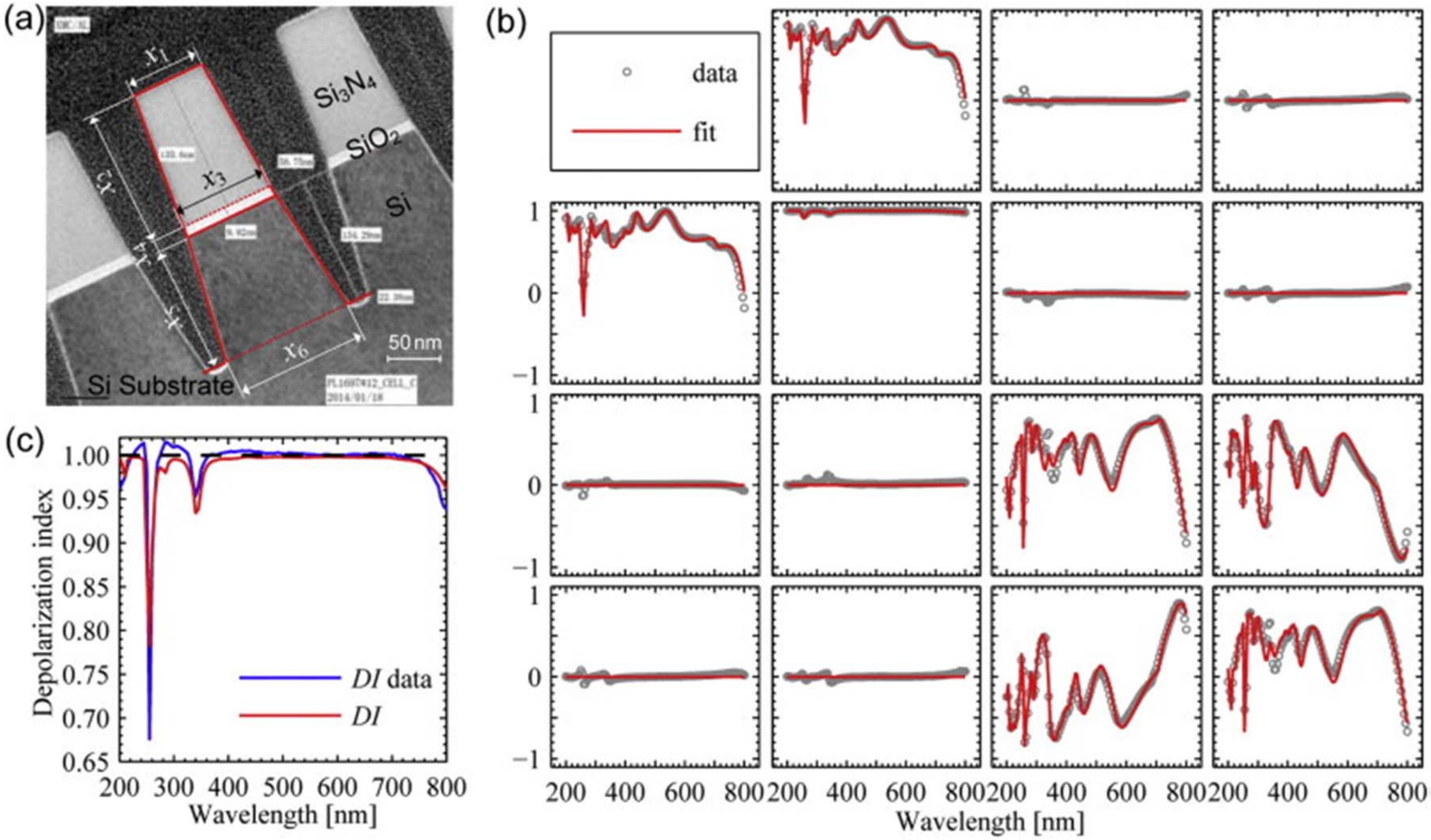

S. Liu, et al., Development of a broadband Mueller matrix ellipsometer as a powerful tool for nanostructure metrology, Thin Solid Films , in press

Helicoidal Bragg reflectors

Cholesteric liquid crystal

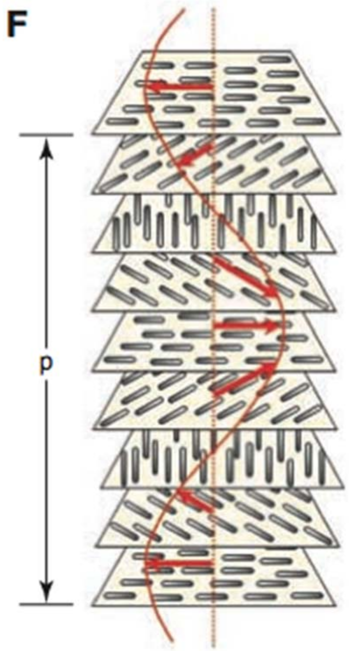

$$\lambda_0 = n_{Average} \cdot p$$
$$\lambda_{peak} = \lambda_0 \cos\theta_i$$
$$\Delta\lambda = p\Delta n$$
$$\Delta n = \left(n_{slow} - n_{fast}\right)$$

Classical approximate formulas for Bragg reflection from cholesteric liquid crystals

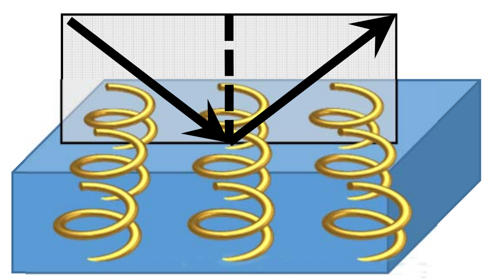

Structural chirality, no real magneto-electric origin.

Helicoidal Bragg reflectors

$$\mathbf{M} = \begin{bmatrix} 1 & m_{01} & m_{02}* & m_{03} \\ m_{01} & m_{11} & m_{12}* & m_{13} \\ -m_{02}* & -m_{12}* & m_{22} & m_{23} \\ m_{03} & m_{13} & -m_{23}* & m_{33} \end{bmatrix}$$

Macraspis lucida

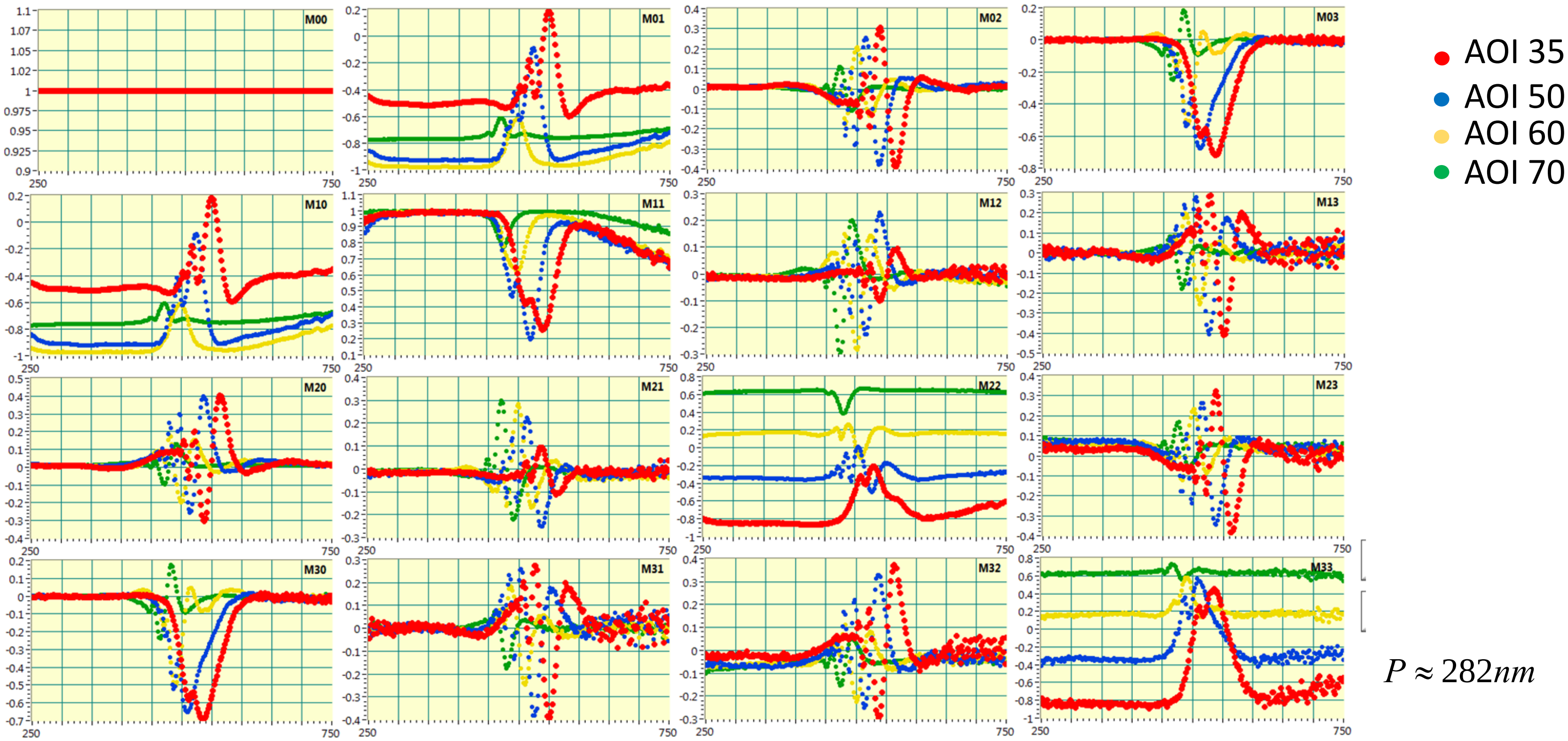

$P \approx 282nm$

Helicoidal Bragg reflectors

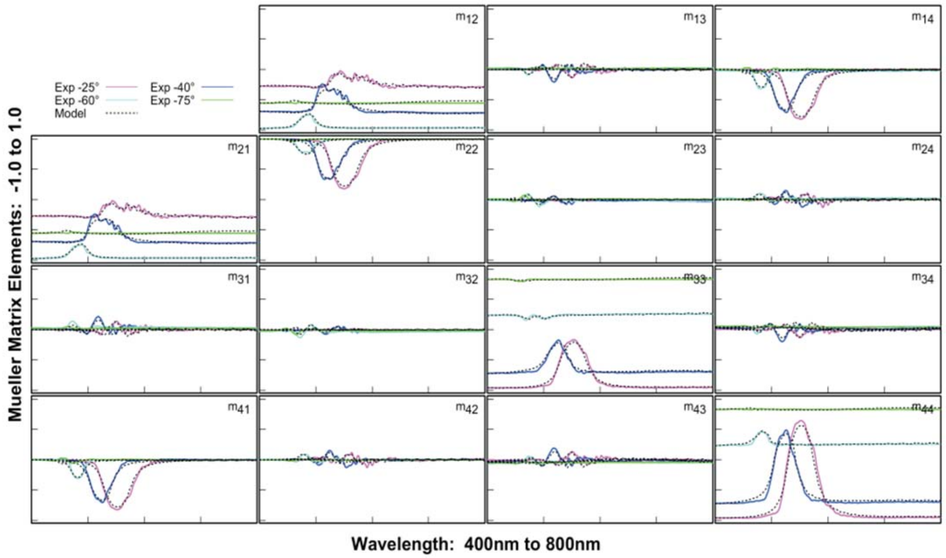

Fig. 5. Mueller-matrix spectra (solid curves) at $\theta = 25°, 40°, 60°$ and $75°$ measured on a green-colored *C. aurata*. The dashed curves show model-generated spectra using the model in Fig. 3. Only data for $\theta = 25°, 40°$ and $60°$ are used in the regression analysis whereas the model data for $\theta = 75°$ are predicted.

H. Arwin et al. Opt. Express **21**, 22645-22656 (2013).

H. Arwin, et al. Opt. Express **23**, 1951-1966 (2015).

$$\mathbf{M} = \begin{bmatrix} 1 & m_{01} & m_{02}* & m_{03} \\ m_{01} & m_{11} & m_{12}* & m_{13} \\ -m_{02}* & -m_{12}* & m_{22} & m_{23} \\ m_{03} & m_{13} & -m_{23}* & m_{33} \end{bmatrix}$$

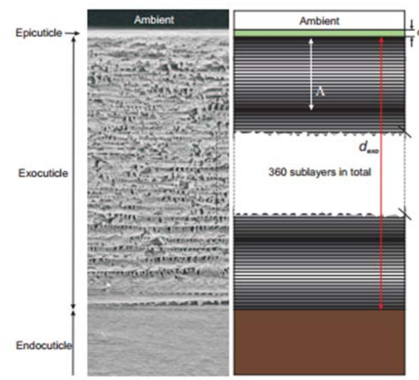

Plasmonic nanostructures

Typically measurements are made on 2D periodic nanostructures with characteristic dimensions comparable or smaller than the wavelength of light

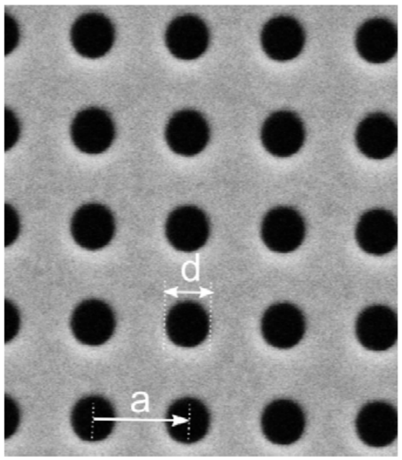

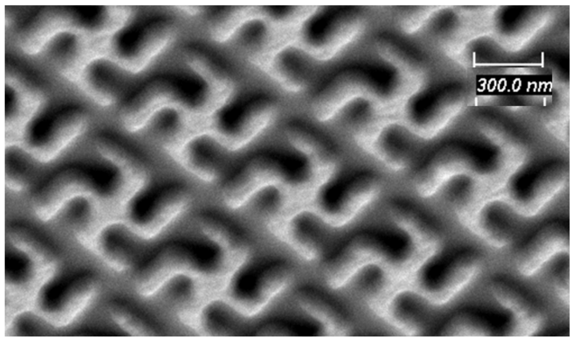

d= 250 nm
a= 530 nm

Big spatial dispersion effects

$$D_i = \varepsilon_{ij}(\omega, \mathbf{k}) E_j \qquad \sim \frac{a}{\lambda}$$

The electric polarization at a certain position is determined not only by the electric field at that position, but also by the fields at its neighbors

…. And the neighbors change depending on how we orient the sample in the ellipsometer….

Plasmonic nanostructures

Projections of a square lattice

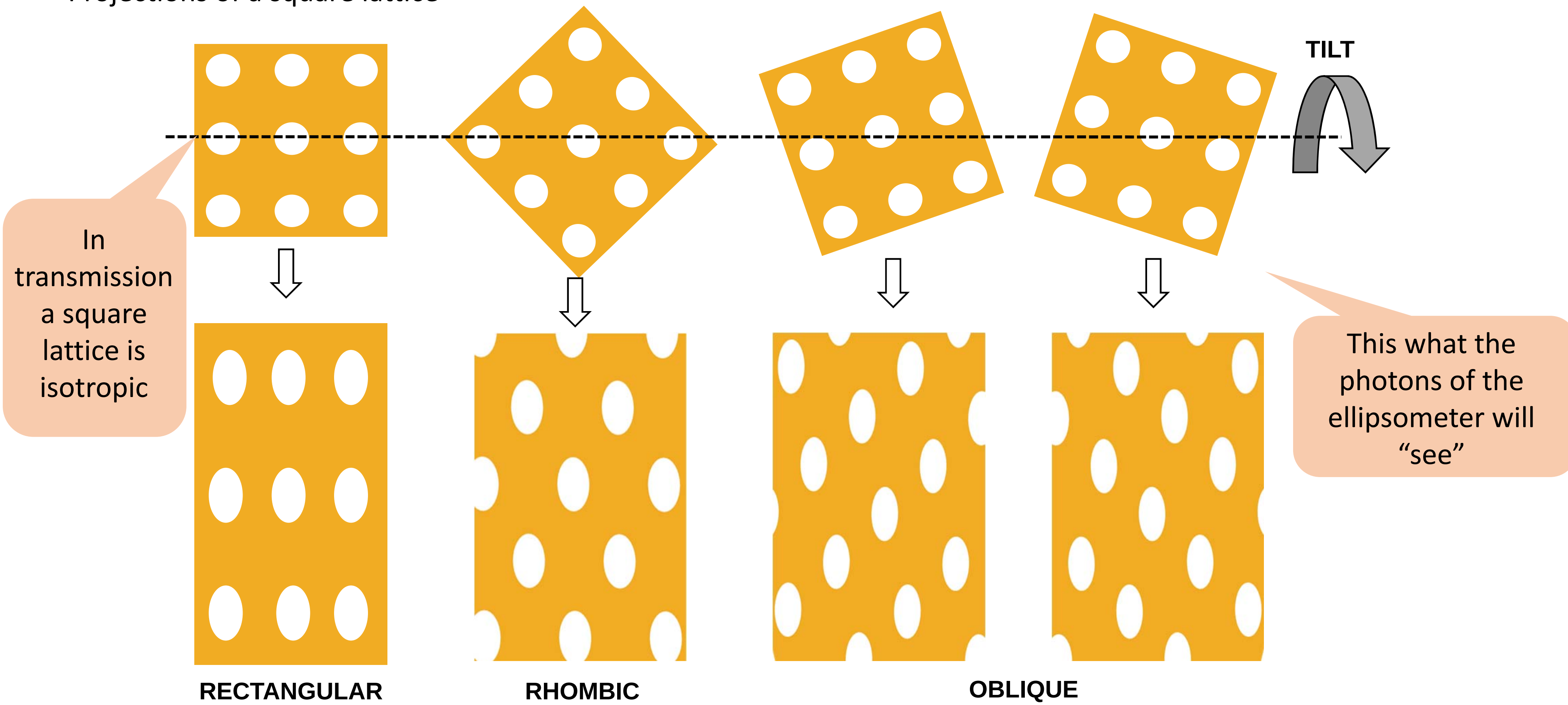

Plasmonic nanostructures

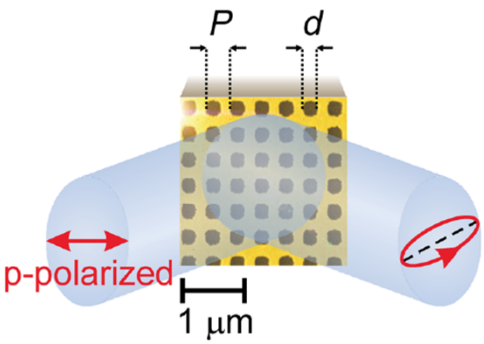

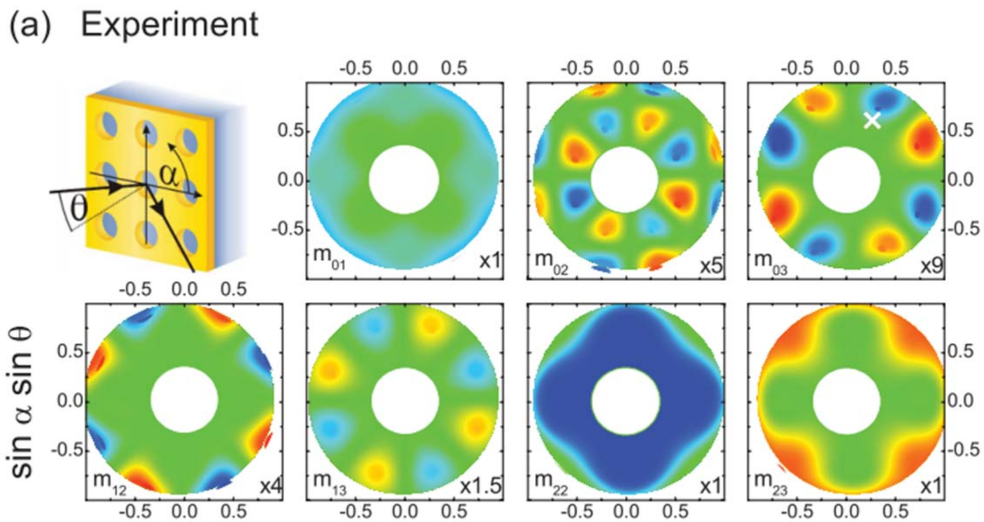

B. Gompf et al. Phys. Rev. Lett. 106, 185501 (2011)

Plasmonic nanostructures

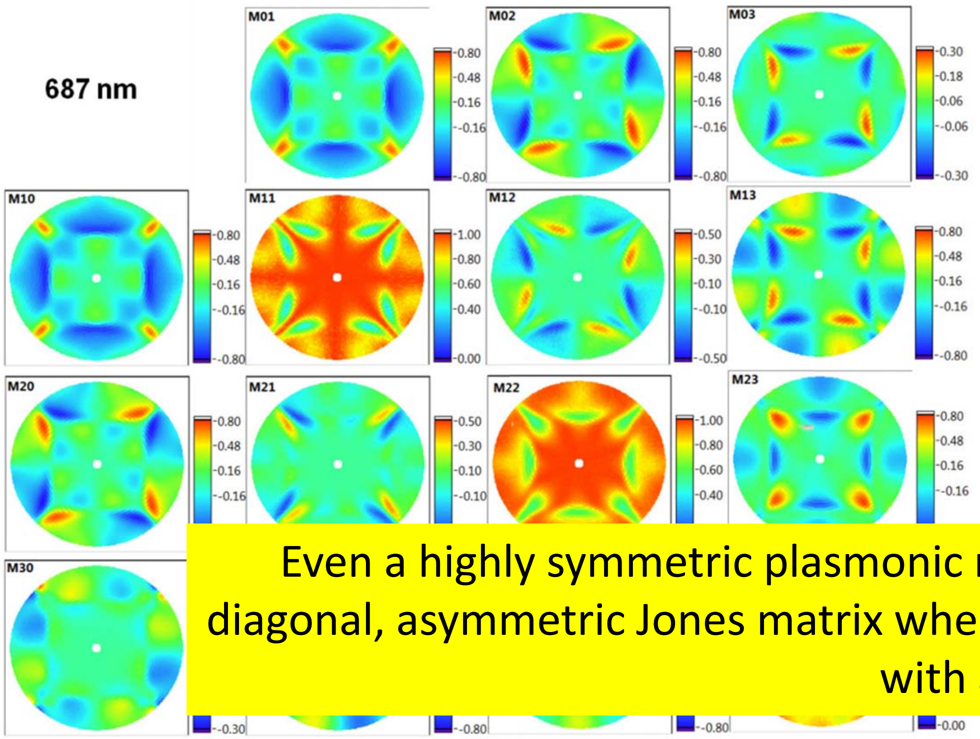

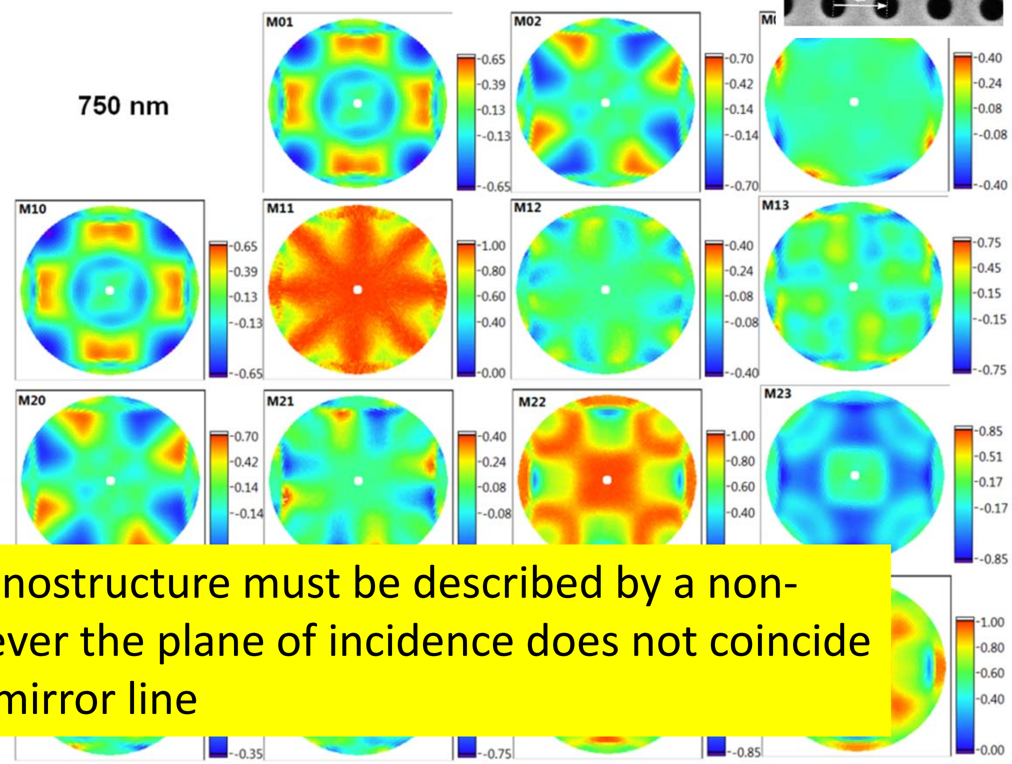

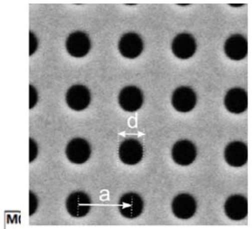

Even a highly symmetric plasmonic nanostructure must be described by a non-diagonal, asymmetric Jones matrix whenever the plane of incidence does not coincide with a mirror line

O. Arteaga, et al., *Opt. Express.*, **22**, 13719, (2014)

Concluding remarks

I have a isotropic sample, should I study with Mueller matrix ellipsometry?

Yes, it never hurts. Having access to the whole MM also helps to verify the alignment of the sample.

I have an anisotropic sample, can I study it with standard ellipsometry?

Most likely yes, although Mueller matrix ellipsometry is arguably better suited.
Reorientations are going to be necessary. Will fail if there is some significant depolarization

I have an optically active sample, can I study it with standard ellipsometry? And with Mueller ellipsometry?

Not with standard ellipsometry. Possibly with Mueller ellipsometry. But be aware! In reflection you will be NOT measuring directly optical rotatory dispersion or circular dichroism.

Summary of ideas to take home

$$\mathbf{M} = \begin{bmatrix} m_{00} & m_{01} & m_{02} & m_{03} \\ m_{10} & m_{11} & m_{12} & m_{13} \\ m_{20} & m_{21} & m_{22} & m_{23} \\ m_{30} & m_{31} & m_{32} & m_{33} \end{bmatrix}$$

- When posible (small depo) convert a experimental MM in a Mueller-Jones matrix or a Jones matrix and work from that
- Symmetries or assymetries of a MM give information about the orientation the sample and/or the crystallographic system
- For intrinsic anisotropy the non-diagonal Jones elements are small and the Mueller matrix is close to a NSC matrix. If they are large suspect about structure-induced anisotropy or misalignement of the sample
- Mueller matrix ellipsometry has the same applications as standard ellipsometry, plus it handles accurately anisotropy and depolarization. Important for crystals, nanotechnology, scatterometry, etc

Some further references

MM symmetries

- O. Arteaga, Thin Solid Films 571, 584-588 (2014)
- H. C. van de Hulst, Light scattering by small particles, New York, Dover (1981)

DF of low symmetry crystals

- G. E. Jellison et al., Phys Rev. B 84, 195439(2011)
- MI Alonso et al., Thin Solid Films 571, 420-425 (2014)
- G. E. Jellison et al. J. Appl. Phys. 112, 063524 (2012)

MMs at normal incidence transmission

- R. Ossikovski, Opt. Let. 39,2330-2332 (2011).
- O. Arteaga et al, Opt. Let. 35, 559-561 (2010)
- J. Schellman, Chem. Rev., 87, 1359-1399 (1987)

MMs at normal-incidence reflection

- O. Arteaga et al. Opt. Let. 39, 6050-6053 (2014)

MM scatterometry

- A. De Martino et al., Proc. SPIE 6922, 69221P (2008).
- S. Liu, et al., Development of a broadband Mueller matrix ellipsometer as a powerful tool for nanostructure metrology, Thin Solid Films , in press

MM and metamaterials

- T. Oates et al., Opt. Mat. Expr. 2646, 2014.

Acknowledgments

R. Ossikovski (EP), A. Canillas (UB),
S. Nichols (NYU) , G. E. Jellison (ORNL)

MARIE CURIE ACTIONS

HINDS INSTRUMENTS

oarteaga@ub.edu
http://www.mmpolarimetry.com